Hybrid labyrinthine-based metamaterials for low-frequency noise attenuation

Abbas Dalvand

K.N. Toosi University of Technology

a.dalvand@email.kntu.ac.ir

Reza Hedayati

K.N. Toosi University of Technology

rezahedayti@kntu.ac.ir

Aliasghar Jafari

K.N. Toosi University of Technology

ajafari@kntu.ac.ir

Abstract

This work introduces a new method for mitigating unwanted sound in manufacturing environments that require solutions with minimal size and mass. The approach utilizes specially engineered acoustic metamaterials, which are both cellular and graded, to achieve superior performance. Compared to a standard hollow cylinder, these developed structures improve sound-blocking capabilities by approximately 40 decibels. Their resonance behavior is also enhanced, with the initial resonant response starting at a frequency 400 Hz lower. Furthermore, the materials display an exceptional capacity for absorbing sound, with measured coefficients of 0.7 and 0.8 in the difficult low-frequency spectrum of 200 Hz to 250 Hz. Weighing about 30 grams and measuring only one centimeter thick, this technology provides a powerful and practical technique. It is highly effective for insulating against low-pitched sounds, particularly in applications where both weight and space are primary concerns.

Keywords: sound, Metamaterial, labyrinthine, low-frequency, thin, light-wight

1. Introduction

Within a time span of 25 years, acoustic metamaterials have emerged from academic curiosity to become an active field driven by scientific discoveries and diverse application potentials [1, 2]. Acoustic metamaterials (AMs) are artificial structures composed of subwavelength units capable of controlling sound wave propagation in a way not achieved by conventional materials [3]. The key feature of AMs is that they have exotic properties not found in nature, including effective negative mass density, negative modulus, or double negative parameters [4-6] which make AMs show significant properties in sound absorption and sound transmission loss [7]. These properties, sound absorption and sound transmission loss, are major parameters in noise controlling [8-10]. When, sound-insulating materials need to increase the thickness or the mass due to the limitations imposed by the mass law [11], and Sound-absorbing materials require the thickness beyond a quarter of the wavelength of the incident sound [12]. While increasing the thickness of both types of the materials can enhance the attenuation in low- frequency ranges, this approach is not the best solution for the purpose of low-frequency noise reduction, and AMs can address this problem [13].

Several types of AMs have proposed include membrane type [14, 15], inherited Helmholtz resonator [16-19], labyrinthine [20, 21] etc. Researchers use them to reach interest sound absorption coefficient and sound transmission loss [22]. However, two topics still are challenging for researchers, these metamaterials not only should be light and thin, but also should address to low frequency noise which is so hard to control with conventional material [23]. So, researchers lead to use combination of different types of materials to overcome these issues. Such as, combination of labyrinthine and Helmholtz resonator [24], plate type and Helmholtz [25], Helmholtz and membrane type [26], and labyrinthine and membrane-type [27].

As labyrinthine show significant acoustic properties and capability to construct in thin cases [28], in same time due to the convenient of Helmholtz structure and its amazing tunable sound absorption and transmission loss capability. The combination of them become a cutting-edge research to control low frequency noise with thin and compacted model [29]. This technique seems applicable for noise attenuation, because has dynamic effect on sound propagation and provide opportunity to produce noise attenuation in thin spaces for reducing noise in automobile cabin and other industry places [17, 30].

This research introduces an innovative technique for managing acoustics by merging the principles of Helmholtz resonance with maze-like pathways. The resulting models were specifically created to overcome critical scientific hurdles in their field by being engineered for minimal thickness and mass. They provide exceptional performance in dampening and blocking low-pitched sound waves.

Two distinct configurations were developed to explore this concept. The initial version is a cellular arrangement, where each individual cell in the structure operates as a discrete resonator. Building on this, a more advanced graded acoustic metamaterial was developed. This second version maintains the labyrinthine form but contains a series of resonators with progressively changing neck dimensions.

The application of these cellular and graded labyrinthine designs for sound management represents a new contribution. While graded designs are a known concept in the mechanical metamaterial domain[31]. their use in this manner is novel. These properties make the structures exceptionally well-suited for deployment in environments dominated by low-frequency acoustic disturbances, such as within vehicles and railcars, where their benefits are most impactful.

2. Materials and methods

2.1. Theories

To evaluate a material's performance in managing noise, two central metrics are essential: its capacity for sound absorption and its effectiveness at impeding sound transmission. Sound absorption specifically relates to a material's ability to dissipate acoustic energy. This process usually involves the transformation of sound waves into another form, most commonly heat. A specific value, the sound absorption coefficient, is used to quantify this characteristic. This coefficient, denoted by the Greek letter, α, is a scalar value that exists on a scale from 0 to 1. Its precise calculation can be performed with the acoustic impedance formula, as presented in equation 1 from reference [32].

$$\alpha = 1 - |\lambda|^2 = 1 - \left|\frac{Z-\rho_0 c_0}{Z+\rho_0 c_0}\right|^2 \quad (1)$$

where λ represents the reflection coefficient, Z denotes the normal acoustic impedance, and ρ_0 and c_0 correspond to the density of air and the speed of sound in air, respectively. The values of ρ_0 and c_0 are typically $1.21\ Kg/m^3$ and $343\ m/s$.

Sound transmission loss is parameter that show how much acoustic energy dissipation from transferring of the material. The transfer matrix methods develop for calculating the sound transmission parameter, where it is shown;

$$\begin{bmatrix} P_b \\ u_b \end{bmatrix}_{x=0} = \begin{bmatrix} T_{11} & T_{12} \\ T_{21} & T_{22} \end{bmatrix} \begin{bmatrix} P_b \\ u_b \end{bmatrix}_{x=d} \tag{2}$$

$$T = \begin{bmatrix} \frac{p_d u_d + p_0 u_0}{p_0 u_d + p_d u_0} & \frac{{p_0}^2 - {p_d}^2}{p_0 u_d + p_d u_0} \\ \frac{{u_0}^2 - {u_d}^2}{p_0 u_d + p_d u_0} & \frac{p_d u_d + p_0 u_0}{p_0 u_d + p_d u_0} \end{bmatrix} \tag{3}$$

That x is position of incidence wave and d is position of end of way. When the parameters are;

$$p_0 = A + B \qquad p_d = Ce^{-jkd} + De^{+jkd} \tag{4}$$

$$u_0 = (A - B)/\rho c \qquad u_d = (Ce^{-jkd} - De^{+jkd})/\rho c \tag{5}$$

$$A = j\frac{H_{1,ref}e^{-jkl_1} - H_{2,ref}e^{-jk(l_1+s_1)}}{2sin\, ks_1} \tag{6}$$

$$B = j\frac{H_{2,ref}e^{+jk(l_1+s_1)} - H_{1,ref}e^{+jkl_1}}{2sin\, ks_1} \tag{7}$$

$$C = j\frac{H_{3,ref}e^{+jk(l_2+s_2)} - H_{4,ref}e^{+jkl_2}}{2sin\, ks_2} \tag{8}$$

$$A = j\frac{H_{4,ref}e^{-jkl_2} - H_{3,ref}e^{-jk(l_2+s_2)}}{2sin\, ks_2} \tag{9}$$

In the equations, p represents pressure, and u denotes particle velocity. H corresponds to the sound reference at four distinct locations: positions 1 and 2 are situated before the specimen, while positions 3 and 4 are located after the specimen. The parameters l_1 and l_2 represent the distances between the sound reference measurements and the specimen, they are shown in Figure 3(d), measured respectively before and after it. Similarly, s_1 and s_2 denote the separation distances between the sound measurements conducted before and after the specimen, respectively.

Correspondingly, the parameter of sound transmission loss (STL) and acoustic impedance calculated;

$$STL = 20log_{10}\left|\frac{1}{t}\right| \tag{10}$$

$$t = \frac{2e^{jkd}}{T_{11} + (T_{12}/\rho c) + \rho c T_{21} + T_{22}} \tag{11}$$

$$Z = \sqrt{T_{12}/T_{21}} \quad (12)$$

As illustrated in Figure 1, the standard model for sound transmission loss (STL) is understood as having three separate regions, each governed by a distinct physical mechanism [33].

Initially, the material's stiffness is the controlling factor. The second zone is characterized by resonance phenomena, which are centered around the angular frequency $\omega = \sqrt{k_{eff}/m_{eff}}$ where k_{eff} and m_{eff} denote the effective stiffness and effective mass, respectively. Beyond the resonance region, the third section's behavior adheres to the mass law. This principle is described by the formula $STL = 10\log\left(1 + (\omega m/(2\rho_c\, c))^2\right)$, where m represents mass, ρ_c is the density of the medium[34, 35].

a)

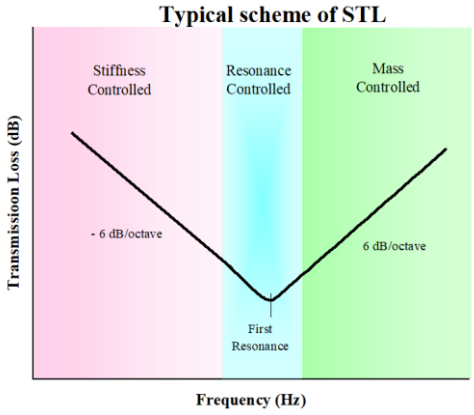

b)

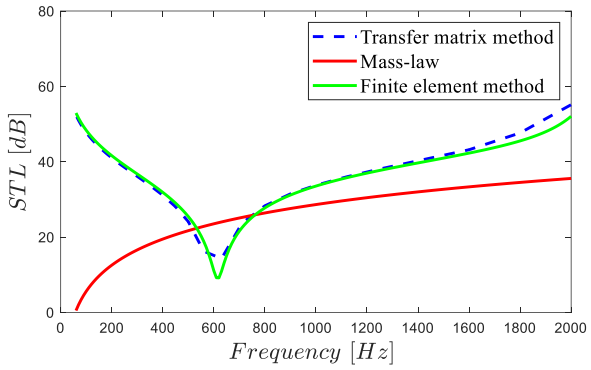

Figure 1 . Typical scheme of normal-incidence STL for a single panel[33]. b) Sound transmission loss verification of 4mm PLA

2.2. Numerical

To evaluate the acoustic absorption capabilities of the cellular and gradient designs, a finite element analysis was conducted using the COMSOL Multiphysics 6.2 software package. This investigation centered on simulating the travel of sound pressure waves through a single unit cell. The pressure acoustics module within the software was selected for the task. Air was established as the acoustic environment for the simulation, with its physical characteristics defined as a mass density of 1.2 kg/m³, sound speed of 343 m/s, and dynamic viscosity of 1.8×10^{-5}Pa·s. The distribution of sound pressure inside the maze-like channel was calculated by numerically solving the Helmholtz equation.

Specific boundary conditions were required to complete the model setup. A port condition, placed at the central aperture on the structure's front face, served as the boundary for the incoming sound wave. Conversely, the terminating end of the model was assigned a non-reflecting boundary condition to prevent wave reflections.

$$\nabla.\left(\frac{-1}{\rho_0}\nabla p\right) - \frac{\omega^2}{\rho_0 {c_0}^2} = 0 \quad (13)$$

Here, ∇ denotes the gradient operator, and pp represents the sound pressure. The absorption coefficient and sound transmission loss were numerically calculated using the following equations:

$$\alpha = 1 - |R|^2 \quad (14)$$

$$STL = 10log_{10}\left(\frac{P_{in}}{P_{out}}\right) \quad (15)$$

In this context, the variable R signifies the reflection coefficient, which is calculated from the established port boundary conditions. The terms W_{in} and W_{out} are used to represent the total acoustic power at the inlet and outlet ports of the model, respectively.

A plot featured in Figure 1(b) offers a comparison between the Finite Element Method (FEM) and the Transfer Matrix Method. It demonstrates the similarity in results when these two approaches are used to analyze a straightforward polylactic acid (PLA) sample measuring 4 mm in thickness and 100 mm in diameter. The graph further serves to illustrate the applicability of the mass law in this situation. For the analysis, the PLA material was defined by properties obtained from experimental tensile tests, including a density of 1250 kg/m^3, a Young's modulus of 699 MPa, and a Poisson's ratio of 0.35.

2.3. Model

A slender structure with an overall thickness of 10 mm was developed for this analysis, as illustrated in Figure 2(a). This model is composed of 1-mm top and bottom layers that enclose an 8-mm thick labyrinthine core. The core's interior contains two separate pathways with consistently 1-mm-thick walls. Sound enters these passages through a pair of 5-mm diameter circular inlets. This specific arrangement is highly effective for absorbing low-frequency sound and improves sound transmission loss by introducing a greater number of resonances.

In a separate analysis, four types of cellular models were investigated: hexagonal, square, re-entrant, and re-hexagonal. Each cell was designed to function as an individual Helmholtz resonator based on

its shape. To create a consistent basis for comparison, all four cell types were constructed with an identical total volume, and the dimensions of their internal cavities and necks were standardized at 3 mm. This standardized design yielded excellent results for the sound absorption coefficient. Table 1 provides schematics for each of the four cellular geometries.

a)

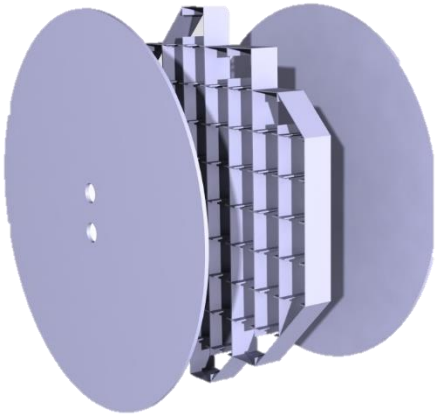

b)

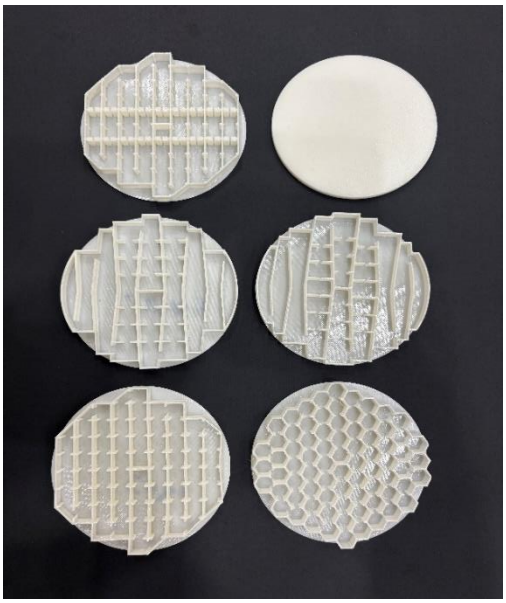

c)

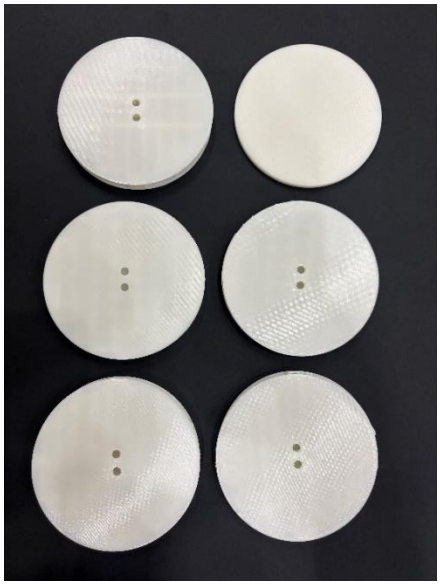

Figure 2. (a) Schematic illustration of the lightweight and thin labyrinthine models along with their structural components. (b) specimens (c) Assembled specimens prepared for testing in the impedance tube.

For the graded labyrinthine models, a novel design strategy was implemented where changes in cell volume were introduced by angling the internal partitions, while a consistent wall thickness was maintained throughout. This created a geometric gradient along the path of sound propagation. Two primary categories were established based on this volume gradient: a "CD" configuration, where cell volume diminishes from the center towards the outer edge, and a "CI" configuration, where it expands radially outward. This smooth transition in cell volume was controlled by a precise angular increment of 4.32 degrees between sections.

In addition to cell volume, the geometry of the connecting necks was methodically altered to assess its impact on acoustic behavior. Three distinct neck profiles were created: a uniform 5 mm width (NS), a decreasing width that tapers from 6 mm to 1 mm (ND), and an increasing width that expands from 1 mm to 6 mm (NI). Combining these three neck profiles with the two types of cell volume gradients resulted in the development of six unique graded structures, as outlined in Table 1.

Five specimens were produced for experimental testing in an impedance tube using Fused Deposition Modeling (FDM), a type of additive manufacturing [36, 37]. The samples were printed with polylactic acid (PLA) at 100% infill to ensure solid parts. As seen in Figure 2(c), the fabricated models included the Hexagonal, Square, Multiple Neck, CD-ND, and CI-NS designs. A simple 4-mm-thick PLA cylinder was also created to serve as a control, allowing for the evaluation of the intrinsic transmission loss of the material itself. To facilitate a fair performance comparison, the other models were designed to have approximately the same mass as this simple cylinder, which provides a clearer insight into the sound attenuation effectiveness of the labyrinthine designs. Figure 2(d) displays the final assembled models, ready for testing.

Table 1 the schematics of two kind of labyrinthine metamaterials; graded and cellular

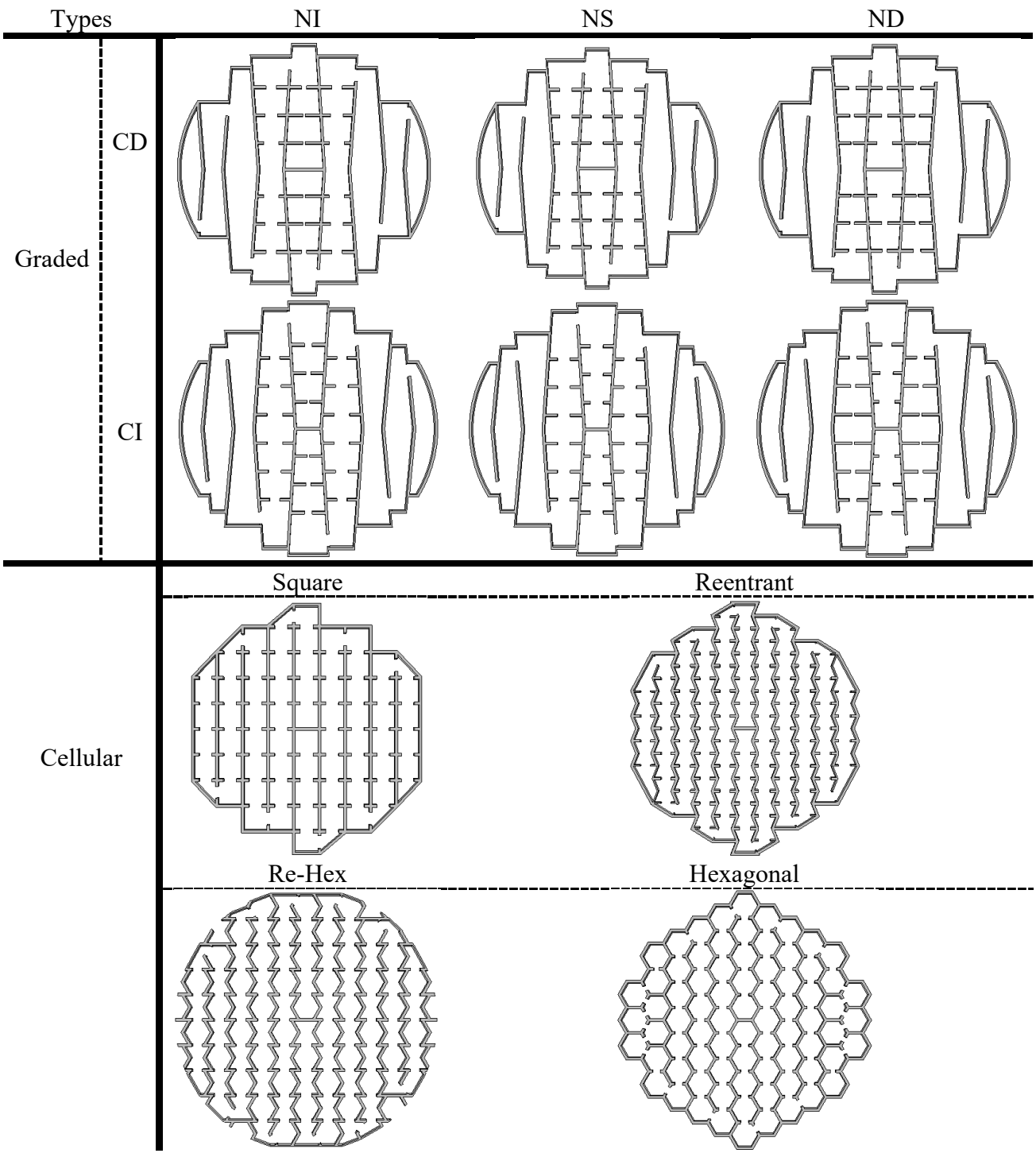

3. Results and discussion

The principal acoustic characteristics of the labyrinthine metamaterials, specifically the sound transmission loss (STL) and the sound absorption coefficient, were validated through physical experiments. These tests were carried out with a BSWA SW422 impedance tube apparatus. For the absorption analysis, specimens with Square, Hexagonal, and CI-ND geometries were created. The STL validation was performed using the CD-NS structure and a basic cylindrical PLA sample.

To measure sound absorption, specimens were positioned within the impedance tube as diagrammed in Figure 3(c). The collected absorption data are plotted in Figure 3(a). A normalization procedure was applied to these data to minimize the effect of background noise from the experimental readings, which allows for a more direct and clear interpretation of the performance.

Initial attempts to measure STL using the setup in Figures 3(d) yielded unexpectedly low and erratic values. An investigation revealed that the sample's outer diameter was slightly under-sized for the tube, which created a poor seal and allowed for undesired air leakages. These flawed experimental data, however, closely matched the outcomes from COMSOL simulations that were modeled with free boundary conditions, mimicking an unsealed state.

To resolve this issue and acquire reliable data, a purpose, built silicone gel gasket was cast to create an airtight seal, as shown in Figure 3(e). This modification successfully replicated fixed boundary conditions inside the tube. The STL test was conducted again with this improved configuration (Figure 3(f)). The new results, presented in Figure 3(b), showed a much stronger correlation with the numerical simulations that appropriately modeled a fixed boundary condition.

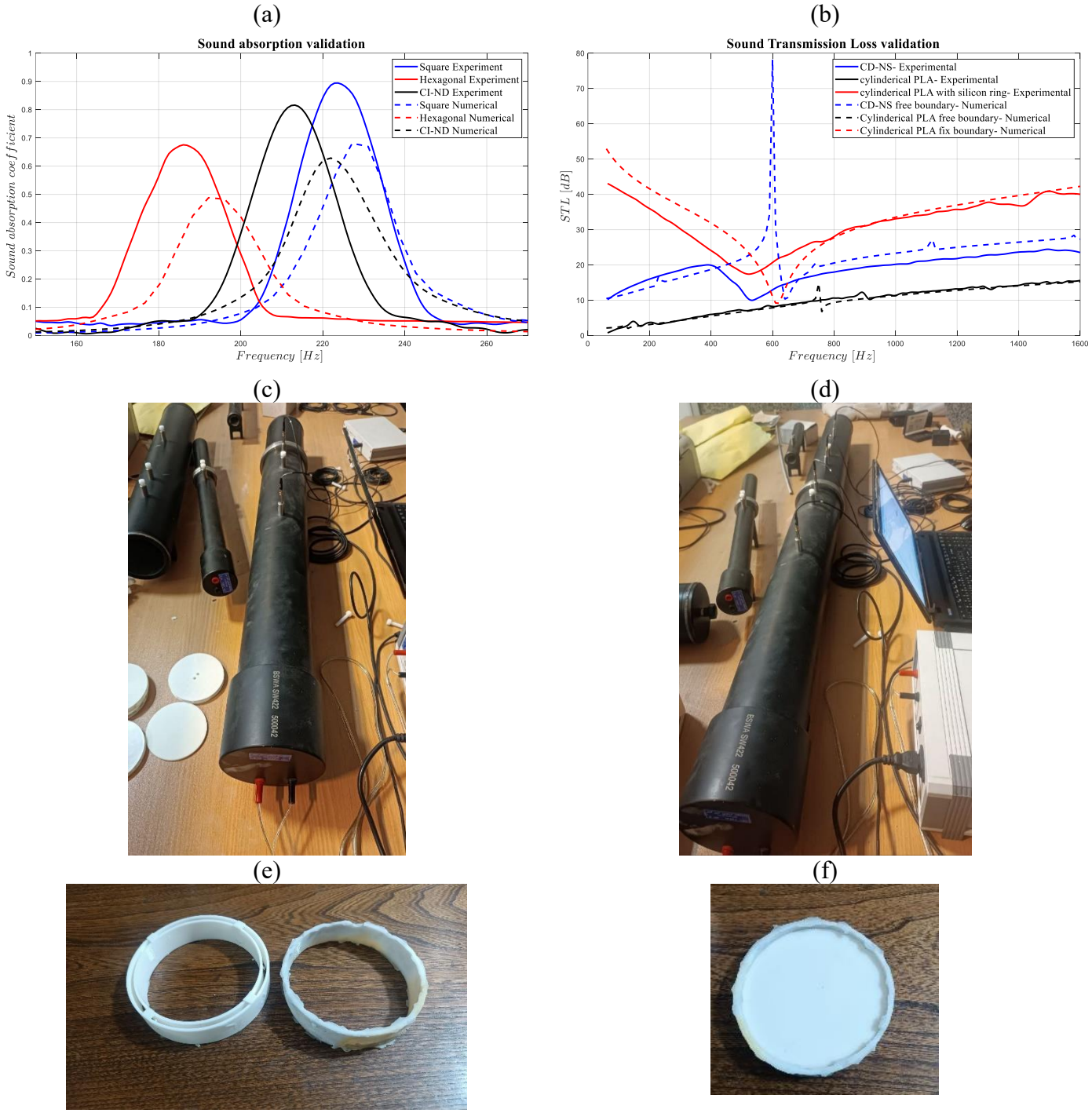

Figure 3. a) Sound absorption coefficient validation b) Sound transmission loss validation c) Impedance tube in absorption setup d) Impedance tube in STL setup e) silicone gel to apply boundary condition for models and it's casting f) Cylindrical PLA with silicon covering for implanting in Impedance tube

4. Discussion

An evaluation was conducted on the fabricated labyrinthine models, contrasting their sound transmission loss (STL) and sound absorption properties against the mass law and a simple rigid PLA specimen of equivalent mass. Both varieties of the labyrinthine structures showed vastly superior STL when compared to the solid PLA cylinder, as seen in Figures 4(b) and 4(d). These models delivered an STL improvement of roughly 40 to 60 dB, an enhancement attributed to how their internal geometry obstructs sound propagation. The structures also exhibit strong low,frequency absorption, which is driven by pronounced thermo-viscous effects arising from the extended acoustic paths and narrow internal channels that dissipate energy.

A detailed look at sound absorption performance is presented in Figure 4(a). The cellular labyrinthine designs showed notable results at low frequencies, with the square model reaching the highest absorption coefficient of approximately 0.7 near 220 Hz, which is linked to its increased thickness. The Re,hex (Reentrant Hexagonal) configuration was also impressive, showing a significant absorption peak of about 0.5 near 180 Hz from a model only 1 cm thick. For the graded designs, illustrated in Figure 4(c), the geometry of the connecting necks was found to be the dominant tuning factor, while changes in cell volume had a negligible influence. This is clear as the neck design (line style) creates substantial differences in absorption, such as the CI,NS model reaching 0.85 at 250 Hz, while the CI,ND model peaks at 0.47 at 220 Hz.

Regarding sound transmission loss, the labyrinthine structures introduced multiple resonances and shifted the primary resonance frequency down from 610 Hz in the simple PLA specimen to approximately 200 Hz, as shown in Figure 4(b). This downward shift significantly boosted STL performance. The Re-hex model had the lowest resonance frequency, resulting in more STL peaks and higher overall transmission loss. Among the graded models, Figure 4(d) shows that graded cell volumes (line style) have a more pronounced effect on STL than neck geometries (color). The CI models consistently performed better at low-frequencies, with the CI-ND specimen reaching an STL of 126 dB at 390 Hz, and the CD,ND model achieving 137 dB at 450 Hz. This highlights that neck modifications optimize absorption while volume gradation enhances sound insulation.

The practical potential of these findings is significant. By strategically combining various configurations, it becomes feasible to achieve broadband sound attenuation within the 180,260 Hz frequency band. This range is highly relevant for tackling common environmental and industrial noise

from sources like vehicles, residential buildings, and offices. Given their exceptionally low weight and compact form, these labyrinthine metamaterials present a promising avenue for developing the next generation of lightweight and space-efficient acoustic insulation solutions.

a)

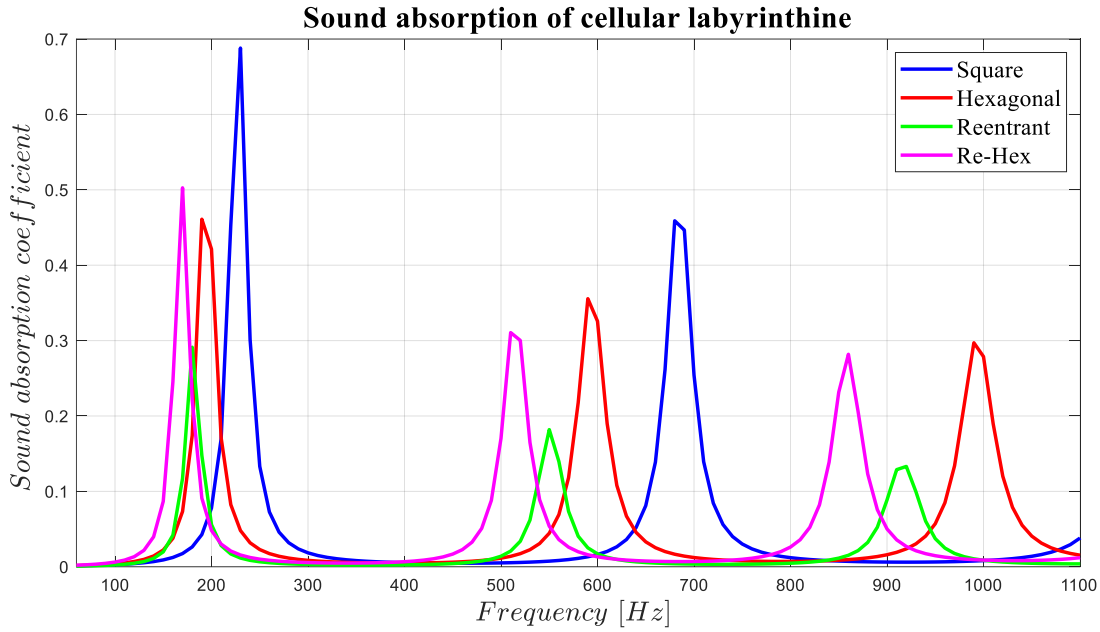

b)

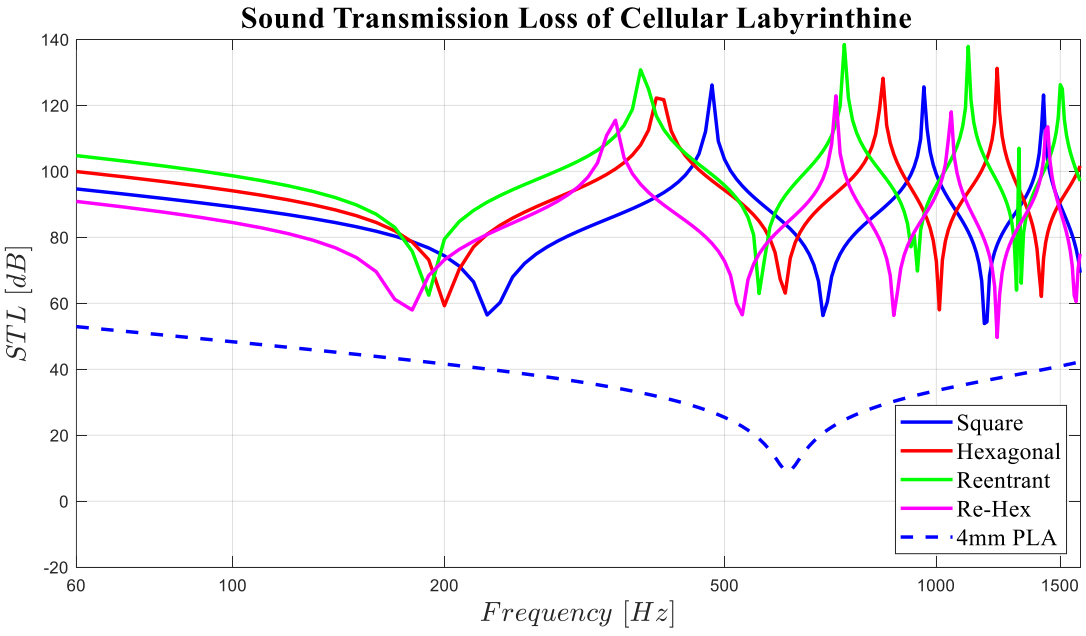

c)

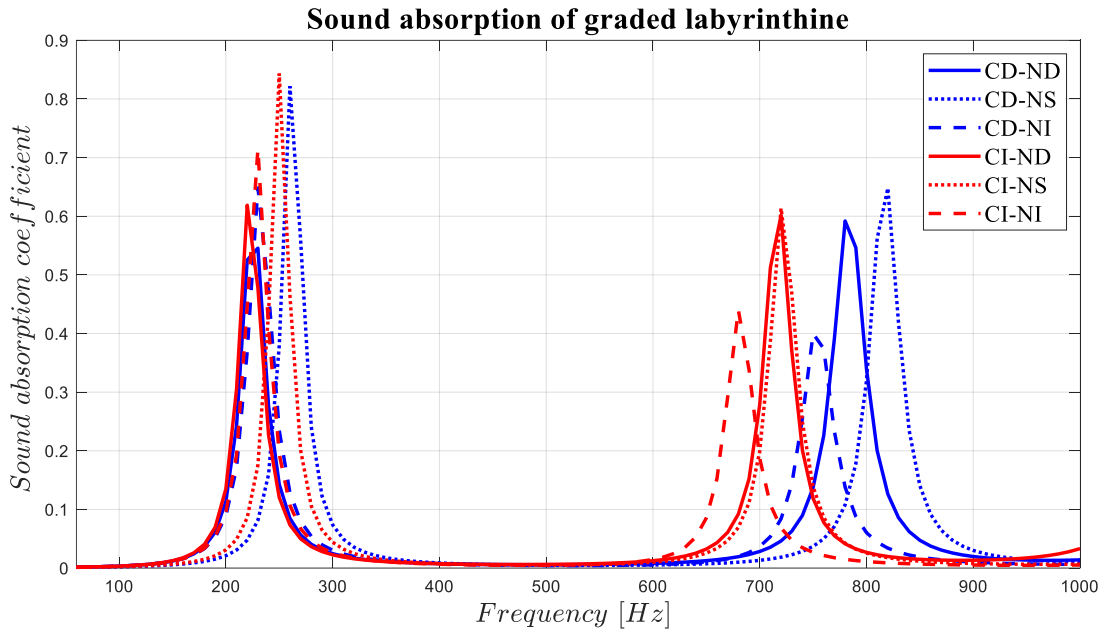

d)

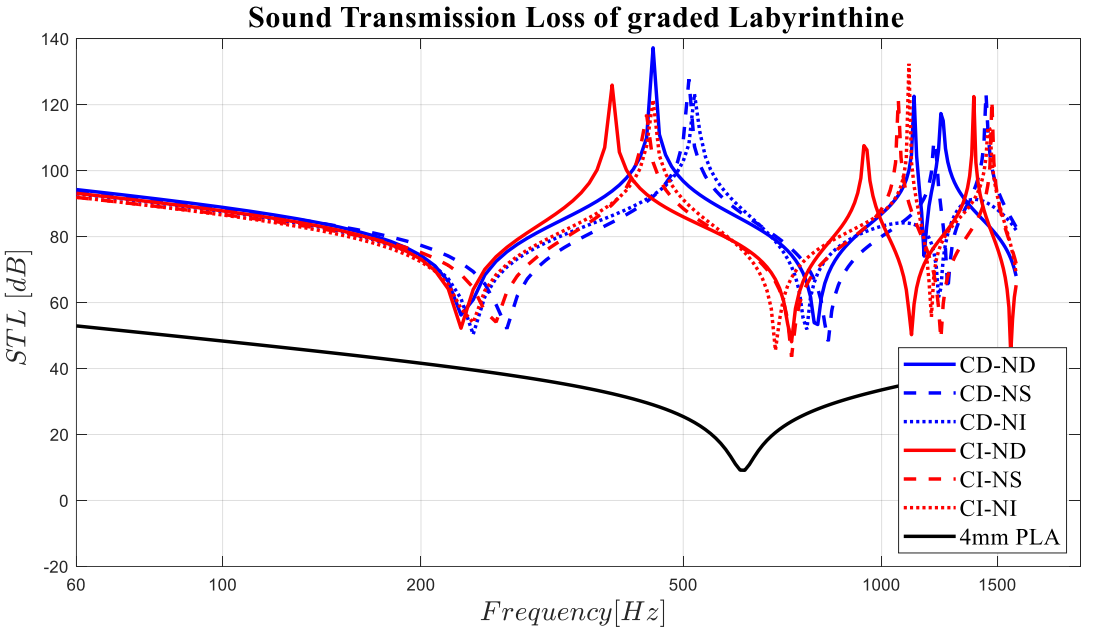

Figure 4. a) Sound absorption plot for cellular configurations b) Sound Transmission Loss logarithm plot for cellular configurations c) Sound absorption plot for graded configurations d) Sound Transmission Loss logarithm plot for graded configurations

This study's findings affirm that labyrinthine metamaterials, in both graded and cellular forms, offer a superior method for insulating against noise, especially in the low-frequency spectrum. The key

conclusion is that despite sharing the same weight (around 30 grams) as a 4-mm-thick solid PLA cylinder, the labyrinthine structures delivered vastly better acoustic performance.

The enhancements were substantial across key metrics. A crucial achievement was shifting the primary resonance frequency down by approximately 400 Hz from the solid PLA model's baseline of 610 Hz. This frequency shift was instrumental in improving sound transmission loss (STL), leading to the creation of multiple insulation peaks over a broader range and resulting in an average STL improvement of about 40 dB. In parallel with this high insulation capability, the metamaterials displayed remarkable sound absorption. Even with a thickness of only 1 cm, most of the tested designs achieved absorption coefficients above 0.4 within the 180–260 Hz range.

This dual performance is particularly significant when compared to traditional acoustic absorbers, which typically need considerable thickness or mass to be effective at low frequencies. The ability of these labyrinthine structures to combine high STL with potent low-frequency absorption in a compact, lightweight package is their defining advantage. Enabled by the design freedom of additive manufacturing, these metamaterials stand out as highly promising candidates for next-generation acoustic treatments in weight-sensitive and space-constrained environments, from automotive applications to residential and office buildings.

4. Conclusion

This work presents a novel strategy for high-performance noise insulation through the design of cellular and graded labyrinthine acoustic metamaterials. The structures were produced from PLA materials using a Fused Deposition Modeling (FDM) additive manufacturing technique, and their performance was confirmed through both COMSOL simulations and physical experiments with an impedance tube.

The results show a remarkable enhancement in acoustic capabilities. Compared to conventional materials of an equivalent weight, the labyrinthine models provide approximately 40 dB greater sound transmission loss. This is achieved in part by fundamentally altering the system's resonance, shifting it downward from a 600 Hz baseline to as low as 180 Hz. Furthermore, the designs exhibit exceptional sound dissipation, achieving absorption coefficients of 0.8 within the low-frequency band of 200 Hz to 300 Hz.

Given their compact 1-cm height and minimal weight of 30 grams, these metamaterials represent an innovative and highly effective solution. They are particularly well-suited for industrial applications that demand powerful low-frequency noise control but are limited by strict spatial and weight constraints.

References

1. Ma, G. and P. Sheng, *Acoustic metamaterials: From local resonances to broad horizons.* Science advances, 2016. **2**(2): p. e1501595.
2. Hedayati, R., N. Ghavidelnia, M. Sadighi, and M. Bodaghi, *Improving the accuracy of analytical relationships for mechanical properties of permeable metamaterials.* Applied Sciences, 2021. **11**(3): p. 1332.
3. Cummer, S.A., J. Christensen, and A. Alù, *Controlling sound with acoustic metamaterials.* Nature Reviews Materials, 2016. **1**(3): p. 1-13.
4. Lee, S.H., C.M. Park, Y.M. Seo, Z.G. Wang, and C.K. Kim, *Acoustic metamaterial with negative density.* Physics letters A, 2009. **373**(48): p. 4464-4469.
5. Fang, N., D. Xi, J. Xu, M. Ambati, W. Srituravanich, C. Sun, and X. Zhang, *Ultrasonic metamaterials with negative modulus.* Nature materials, 2006. **5**(6): p. 452-456.
6. Lee, S.H. and O.B. Wright, *Origin of negative density and modulus in acoustic metamaterials.* Physical Review B, 2016. **93**(2): p. 024302.
7. Shah, S.S., D. Singh, J. Saini, N. Garg, and C. Gautam, *Acoustical Metamaterials for Noise Control Applications*, in *Handbook of Vibroacoustics, Noise and Harshness*. 2024, Springer. p. 835-848.
8. Hong, T.W. and C. Sin, *Sound transmission loss analysis on building materials.* International Journal of Automotive and Mechanical Engineering, 2018. **15**(4): p. 6001-6011.
9. Zwinselman, J. and W. Bachmann, *Polyurethane foams for sound and vibration dampening in automotive applications.* Journal of cellular plastics, 1988. **24**(3): p. 274-283.
10. Hedayati, R. and M.J.A.S. Bodaghi, *Acoustic metamaterials and acoustic foams: recent advances.* 2022. **12**(6): p. 3096.
11. Kumar, S. and H. Lee, *The present and future role of acoustic metamaterials for architectural and urban noise mitigations. Acoustics 2019, 1, 590–607*.
12. Arenas, J.P. and M.J. Crocker, *Recent trends in porous sound-absorbing materials.* Sound & vibration, 2010. **44**(7): p. 12-18.
13. Lee, I., I. Han, and G. Yoon, *Compact acoustic metamaterials based on azimuthal labyrinthine channels for broadband low-frequency soundproofing and ventilation.* Applied Acoustics, 2025. **228**: p. 110273.
14. Mei, J., G. Ma, M. Yang, Z. Yang, W. Wen, and P. Sheng, *Dark acoustic metamaterials as super absorbers for low-frequency sound.* Nature communications, 2012. **3**(1): p. 756.
15. Nguyen, H., Q. Wu, J. Chen, Y. Yu, H. Chen, S. Tracy, and G. Huang, *A broadband acoustic panel based on double-layer membrane-type metamaterials.* Applied Physics Letters, 2021. **118**(18).
16. Jiménez, N., W. Huang, V. Romero-García, V. Pagneux, and J.-P. Groby, *Ultra-thin metamaterial for perfect and quasi-omnidirectional sound absorption.* Applied Physics Letters, 2016. **109**(12).
17. Kong, W., T. Fu, and T. Rabczuk, *Improvement of broadband low-frequency sound absorption and energy absorbing of arched curve Helmholtz resonator with negative Poisson's ratio.* Applied Acoustics, 2024. **221**: p. 110011.
18. Hedayati, R. and S. Lakshmanan, *Pneumatically-Actuated Acoustic Metamaterials Based on Helmholtz Resonators.* Materials, 2020. **13**(6): p. 1456.

19. Hedayati, R. and S.P.J.M. Lakshmanan, *Active acoustic metamaterial based on Helmholtz resonators to absorb broadband low-frequency noise.* 2024. **17**(4): p. 962.
20. Liang, Z. and J. Li, *Extreme acoustic metamaterial by coiling up space.* Physical review letters, 2012. **108**(11): p. 114301.
21. Catapane, G., G. Petrone, O. Robin, and K. Verdière, *Coiled quarter wavelength resonators for low-frequency sound absorption under plane wave and diffuse acoustic field excitations.* Applied Acoustics, 2023. **209**: p. 109402.
22. Hedayati, R., D. Casalino, D. Ragni, S. van der Zwaag, and F. Avallone, *Acoustic Liner.* 2020.
23. Gao, N., Z. Zhang, J. Deng, X. Guo, B. Cheng, and H. Hou, *Acoustic metamaterials for noise reduction: a review.* Advanced Materials Technologies, 2022. **7**(6): p. 2100698.
24. Hu, P., J. Zhao, H. Liu, X. Zhang, G. Zhang, and H. Yao, *Low-Frequency Sound-Insulation Performance of Labyrinth-Type Helmholtz and Thin-Film Compound Acoustic Metamaterial.* Materials, 2024. **17**(18): p. 4475.
25. Li, R.-S., X.-W. Sun, X.-L. Gao, G.-G. Xu, T. Song, and J.-H. Tian, *Sound transmission loss overlay mechanism of plate-type acoustic metamaterials with Helmholtz resonators.* Physics Letters A, 2025: p. 130358.
26. Li, H.-Z., J.-S. Yang, Q. Liu, S. Li, X.-C. Liu, F. Yang, and L.-Z. Wu, *A novel sandwich structure for integrated sound insulation and absorption.* International Journal of Mechanical Sciences, 2024. **279**: p. 109526.
27. Lan, J., Y. Zhou, X. Bu, and Y. Li, *Sound insulation performance of multi-layer membrane-type acoustic metamaterials based on orthogonal experiments.* arXiv preprint arXiv:2502.16123, 2025.
28. Kumar, S. and H. Pueh Lee, *Reconfigurable metatiles with circular maze-like space-coiling-based acoustic metastructure for low-to-mid frequency sound attenuation.* Journal of Applied Physics, 2023. **133**(15).
29. Liu, Y., G. Cao, C. Liu, and F. Ma, *Ultra-thin arc-shaped conformal metasurface coating for broadband noise reduction in underwater pipeline.* Applied Acoustics, 2025. **228**: p. 110314.
30. Jonza, J., T. Yoo, T. Herdtle, J. Kalish, R. Gerdes, and G. Eichhorn. *Acoustically Absorbing Lightweight Thermoplastic Honeycomb Panels*. in *INTER-NOISE and NOISE-CON Congress and Conference Proceedings*. 2017. Institute of Noise Control Engineering.
31. Bodaghi, M., A. Damanpack, and W. Liao, *Adaptive metamaterials by functionally graded 4D printing.* Materials & Design, 2017. **135**: p. 26-36.
32. Kinsler, L.E., A.R. Frey, A.B. Coppens, and J.V. Sanders, *Fundamentals of acoustics*. 2000: John wiley & sons.
33. Sabet, S.M. and A. Ohadi, *Experimental and theoretical investigation of sound transmission loss for polycarbonate, poly (methyl methacrylate), and glass.* Journal of Applied Polymer Science, 2016. **133**(7).
34. Josse, R. and C. Lamure, *Transmission du son par une paroi simple.* Acta Acustica united with Acustica, 1964. **14**(5): p. 266-280.
35. Kong, Y., J. Wen, A. Huang, L. Zhou, and Y. Xiao, *Acoustic properties of glued laminated bamboo and spruce-pine-fir.* Wood Material Science & Engineering, 2023. **18**(5): p. 1765-1779.
36. Hedayati, R., A. Yousefi, M.L. Dezaki, and M.J.j.o.t.m.b.o.b.m. Bodaghi, *Analytical relationships for 2D Re-entrant auxetic metamaterials: An application to 3D printing flexible implants.* 2023. **143**: p. 105938.
37. Roudbarian, N., M. Baniasadi, P. Nayyeri, M. Ansari, R. Hedayati, M.J.S.M. Baghani, and Structures, *Enhancing shape memory properties of multi-layered and multi-material polymer composites in 4D printing.* 2021. **30**(10): p. 105006.